COMPARATIVE STUDIES ON THE DEFORMATION BEHAVIOUR OF FRP AND STAINLESS STEEL-REINFORCED CONCRETE BEAMS WITH A T-SHAPED CROSS-SECTION

Nora S. Tost, University of Kaiserslautern-Landau, Germany, nora.bies@rptu.de
Matthias Pahn, University of Kaiserslautern-Landau, Germany, matthias.pahn@rptu.de

ABSTRACT

In this study, comparative investigations are carried out on GFRP and stainless steel reinforced concrete beams with the same degree of reinforcement in the 4-point bending test. The specimens have a reduced cross-section in the centre of the component and are T-shaped. In addition to displacement transducers, fibre-optic measurement technology is used to map the stress-related bar strain over the length of the component, as well as photogrammetry. The aim is to identify and evaluate the differences in the deformation behaviour of concrete beams with flexural tensile reinforcement made of GFRP and stainless steel.

KEYWORDS

GFRP internal reinforcement; stainless steel; 4-point bending test; deformation behaviour; fibre-optic measurement technology; photogrammetry

INTRODUCTION

In the decades since its invention, the composite material reinforced concrete has become firmly established in the construction industry, as the materials concrete and steel are very complementary. If the tensile strength of the concrete is exceeded, for example in the tensile zone of a component subjected to bending, the steel reinforcement bears the load. The high stiffness of the reinforcing steel ensures that the serviceability limit state values are complied with and thus deflections and crack widths are low, even at low reinforcement ratios.

Nevertheless, the application possibilities of steel reinforced concrete remain limited due to its material-specific properties. On the one hand, reinforced concrete has a very high dead weight, which is not suitable for the realisation of filigree and light construction designs. On the other hand, internal and external influences such as mechanical stress, environmental influences as well as chemical and biological attacks lead to a reduction of the alkaline environment of the concrete. As a result, the corrosion resistance decreases. The durability of a reinforced concrete element depends mainly on the extent to which steel corrosion can be limited or prevented. Therefore, in corrosive environments, stainless steel reinforcement is used instead of reinforcing steel.

Reinforcing bars made of fibre-reinforced plastic (FRP) represent an alternative to conventional reinforcing steel. The modern composite material opens up new perspectives in construction, as it has a high chemical resistance and a low dead weight. Internal FRP reinforcement is particularly suitable for corrosion-promoting environmental conditions. The greatest importance on the market is attached to rebars made of glass-fibre reinforced plastic (GFRP), as glass is considerably cheaper than carbon (Gudonis et al., 2013). With a tensile strength of over 1,000 N/mm^2 and a modulus of elasticity of approximately 60,000 N/mm^2, GFRP reinforcement bars have a higher tensile strength than steel, but at the same time they are considerably softer (Knab et al., 2015; Sayed-Ahmed et al., 2017). When using the innovative GFRP reinforcement, the ultimate limit state is therefore less decisive for the design than the serviceability limit state (Barris et al., 2013). Especially in cracked state, larger deflections and wide crack widths occur.

In this study, comparative investigations are carried out on components reinforced with either stainless steel or GFRP reinforcement in the bending tension zone. The longitudinal reinforcement

ratio is not varied. The components are tested in a 4-point bending test until failure. A fibre-optic measuring system is used to measure the axial strain of the bending tensile reinforcement. The deflection in the centre of the span is measured with an inductive displacement transducer. In addition, photogrammetry is used to measure one side of the specimen during testing.

EXPERIMENTAL PROGRAMME
The scope of experiments includes the investigation of four reinforced specimens and is shown in Table 1. The specimens are beams with a reduced cross-section in the centre of the member, which are reinforced in the bending tension zone with only one rebar with a diameter of 16 mm. For the beams BS1 and BS2, the reinforcement consists of a stainless steel rebar with a nominal diameter of 16 mm, while the beams BG1 and BG2 have a GFRP rebar with a nominal diameter of 16 mm as reinforcement. Table 1 also shows which instrumentation is used in the tests: Inductive displacement transducers (LVDT), fibre optic measurement technology (FO) and photogrammetry (GOM).

Table 1: Experimental progamme

Beam	Material	Number of rebars	Rebar diameter [mm]	Concrete batch	Instrumentation
BS1	Stainless steel	1	16	1	LVDT + FO
BS2		1	16	3	LVDT + GOM
BG1	GFRP	1	16	1	LVDT + FO
BG2		1	16	2	LVDT + GOM

Materials
Stainless steel reinforcement
The stainless steel used is a B500B NR, used in construction where carbonation and moderate chloris exposure is expected.

GFRP reinforcement
The GFRP reinforcement bar is manufactured using the pultrusion process and consists of ECR glass fibres and a vinyl ester resin matrix. After the matrix has hardened, ribs are milled helically into the bar to ensure the bond between the concrete and the reinforcement. The GFRP rebar has a tensile strength of over 1,000 N/mm^2. The modulus of elasticity is 60,000 N/mm^2.

Concrete
The test specimens were produced in three concrete batches. Concrete with a maximum grain size of 8 mm was used. The concrete properties were determined on the day of the experiment by using test cubes and cylinders, which were produced alongside the test specimens with concrete of the same mix. The determination of the compressive strength was carried out according to DIN EN 12390-2 (DIN Deutsches Institut für Normung e. V., 2019), the determination of the tensile splitting strength according to DIN EN 12390-6 (DIN Deutsches Institut für Normung e. V., 2010) and the determination of the modulus of elasticity according to DIN EN 12390-13 (DIN Deutsches Institut für Normung e. V., 2021).

Table 2 gives the results of the concrete test. The mean compressive strength is between 41.6 and 64.8 N/mm^2. Due to the soft aggregates, the concrete has a modulus of elasticity between 22,255 and 30,043 N/mm^2. The tensile splitting strength is between 2.50 and 3.75 N/mm^2. The cubes and cylinders were stored in dry conditions together with the beams.

Table 2: Material properties of the concrete

Concrete batch	Beam	Testing age [d]	Mean compressive strength on dry stored cubes $f_{cm,cube,dry}$ [N/mm^2]	Mean modulus of elasticity E_{cm} [N/mm^2]	Mean tensile splitting strength $f_{ctm,sp}$ [N/mm^2]
1	BS1	29	62.2	28,485	3.50
	BG1	30			
2	BG2	27	41.6	22,255	2.50
3	BS2	44	64.8	30,043	3.75

Beam specifications

The specimen is shown in Figure 1 in the view and in the sections A-A and B-B. The specimen is 1.50 m long, 0.30 m wide and 0.40 m high. In the area of the abutments, the cross-section has a rectangular geometry (see section A-A), while the cross-section in the centre has a reduced T-shape over a length of 1.00 m (see section B-B).
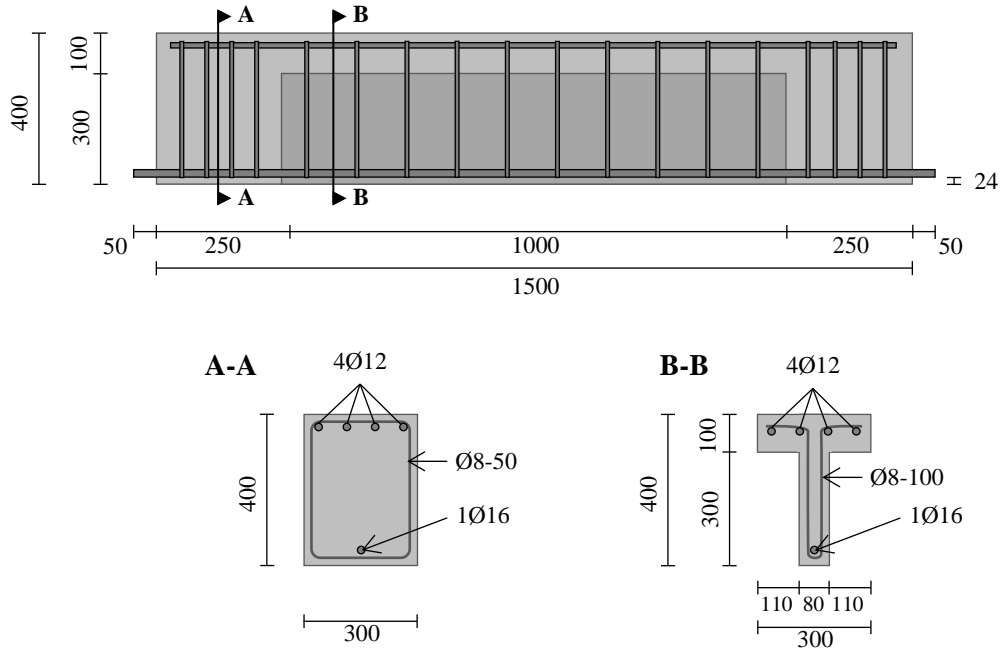

Figure 1: Geometric details of the tested beams (all dimensions in mm)

In the compression zone, the beam is reinforced with four stainless steel rebars with a diameter of 12 mm. In the area of the abutments, the shear reinforcement consists of rectangular stirrups made of stainless steel with a diameter of 8 mm, which are spaced at intervals of 50 mm. In the middle of the beam, where the cross-section has a T-shape, the stirrups are bent into a T-shape, but again 8 mm stainless steel bars are used, which are spaced 100 mm apart. A rebar with a diameter of 16 mm is located in the bending tension zone. According to the test programme, see Table 1, this is varied so that a stainless steel or a GFRP rebar is used. The concrete cover of the bending tension reinforcement is 24 mm, which is 1.5-times the rebar diameter of 16 mm.

Test setup and instrumentation

The beams are tested in a 4-point bending test until failure. The support at the edges of the beam as well as the load introduction construction was designed statically determined. The 1.50 m long beam is loaded in the middle with two concentrated loads by transferring the load of the testing machine via a steel element to two bearings, which have a distance of 200 mm. Figure *2* shows the test setup and the measurement concept schematically.

An inductive displacement transducer is placed at a distance of 700 mm from the abutments. The entire visible surface of the beam is covered with a black and white stochastic pattern for photogrammetry. On the rebar in the bending tension zone, which is the subject of the investigations of this study, a fiber optic sencor is applied over the length of 1.50 m.
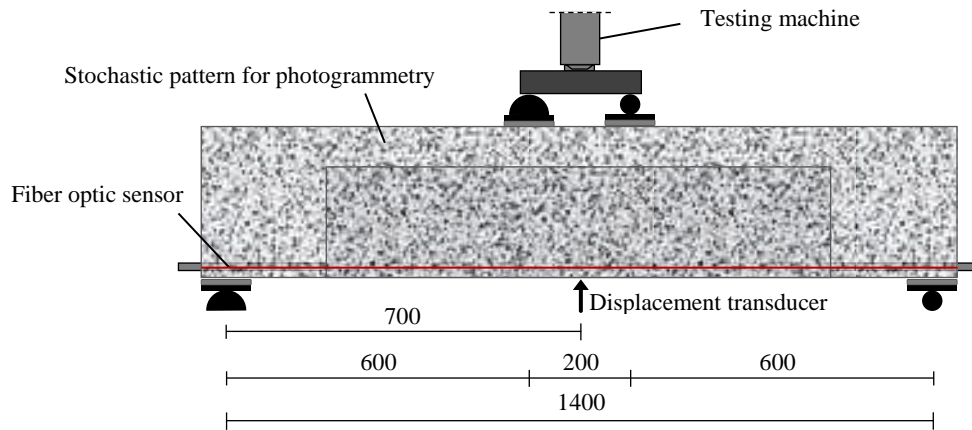
Figure 2: Test setup and instrumentation (all dimensions in mm)

Fibre-optic measurement technology

To determine the strain of the flexural reinforcement, a quasi-continuous fibre-optic technique is used, which is based on the analysis of Rayleigh backscatter. The fiber optic sensor is glued directly onto the surface of the stainless steel reinforcement and glued into a previously milled groove of the GFRP reinforcement. The OdiSI measuring system by LUNA is used. The system allows strain measurements up to ± 12000 με in an interval with a minimum of 0.65 mm.

Photogrammetry

The non-contact measurement method of photogrammetry enables the detection of deformations, cracks and other damages during the experimental testing of specimens and is based on the Digital Image Correlation (DIC) technique. The camera system used is the ARAMIS Adjustable 12M by Carl Zeiss GOM Metrology GmbH. The camera system has a maximum measuring volume of 5000 x 4000 x 4000 mm^3, which corresponds to a volume of 5 m length, 4 m height and 4 m depth. The resolution is 4096 x 3000 pixels. In full screen, measurements can be taken with a maximum frequency of 25 Hz.

In order to capture the measurement points, a stochastic pattern is required and the observed surface of the specimen is painted in advance with white and black paint. As shown in Figure 3, the specimen is primed with white paint in the first step (see Figure 3, left) before the pattern is applied with black paint (see Figure 3, middle). From the stochastic pattern (see Figure 3, right), the system forms individual facets that represent the measurement points.

Figure 3: Priming (left), applying the pattern (middle) and prepared beam with stochastic pattern

TEST RESULTS AND DISCUSSION
Results on deflection
Results of measurement by inductive displacement transducers
Figure 4 shows the deflection in mm in relation to the load in kN for the stainless steel reinforced specimens BS1 and BS2, as well as for the GFRP reinforced specimens BG1 and BG2.
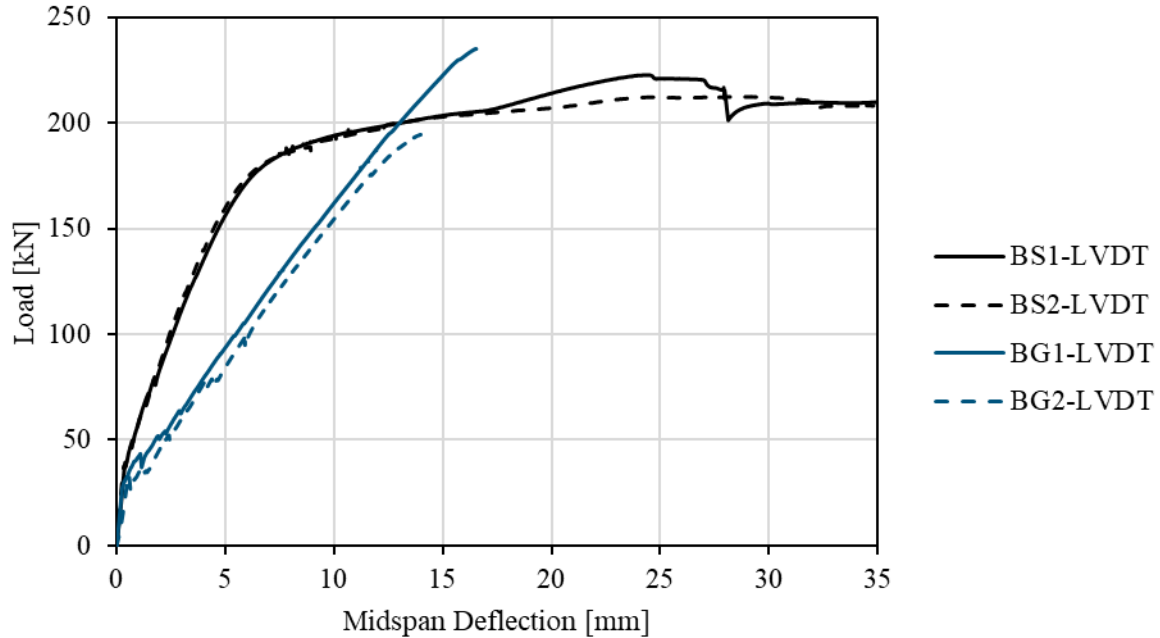

Figure 4: Load-Midspan Deflection relationship measured by displacement transducer (LVDT)

Table 3 shows salient points of the load-deflection relationship: the load at initiation of the initial crack F_{cr} in kN and the related deflection in mm, as well as the maximum load F_u in kN and the related deflection in mm.

Table 3: Initial cracking load, Ultimate load and related midspan deflection of the test beams

Beam	Initial cracking load F_{cr} [kN]	Midspan deflection [mm]	Ultimate load F_u [kN]	Midspan deflection [mm]
BS1	39.29	0.39	222.70	24.29
BS2	37.59	0.33	212.43	28.64
BG1	26.95	0.25	234.99	16.55
BG2	33.70	0.55	194.50	13.99

For beam BS1, the initial crack occurs at a load of 39.29 kN and 0.39 mm deflection. Beam BS2 reaches a maximum load of 212.43 kN at 28.64 mm deflection and the first crack at 37.59 kN and 0.33 mm deflection.
The GFRP-reinforced members show the initial crack at 26.95 kN and 0.25 mm for BG1 and 33.70 kN and 0.55 mm for BG2. The maximum load is highest for BG1 at 234.99 kN and 16.55 mm and lowest for BG2 at 194.50 kN and 13.99 mm.

The plastic properties of the stainless steel reinforcement cause the crack widths to increase after reaching the maximum load and a secondary concrete compression zone failure occurs. Therefore, it was determined that deflections up to 35 mm are shown in Figure 4. The GFRP-reinforced components fail brittly at the maximum load.

As the range up to 80 kN is discussed in more detail in the following chapters, Figure 5 shows the load-deflection diagram from 0 to 100 kN load and 0 to 5 mm deflection.
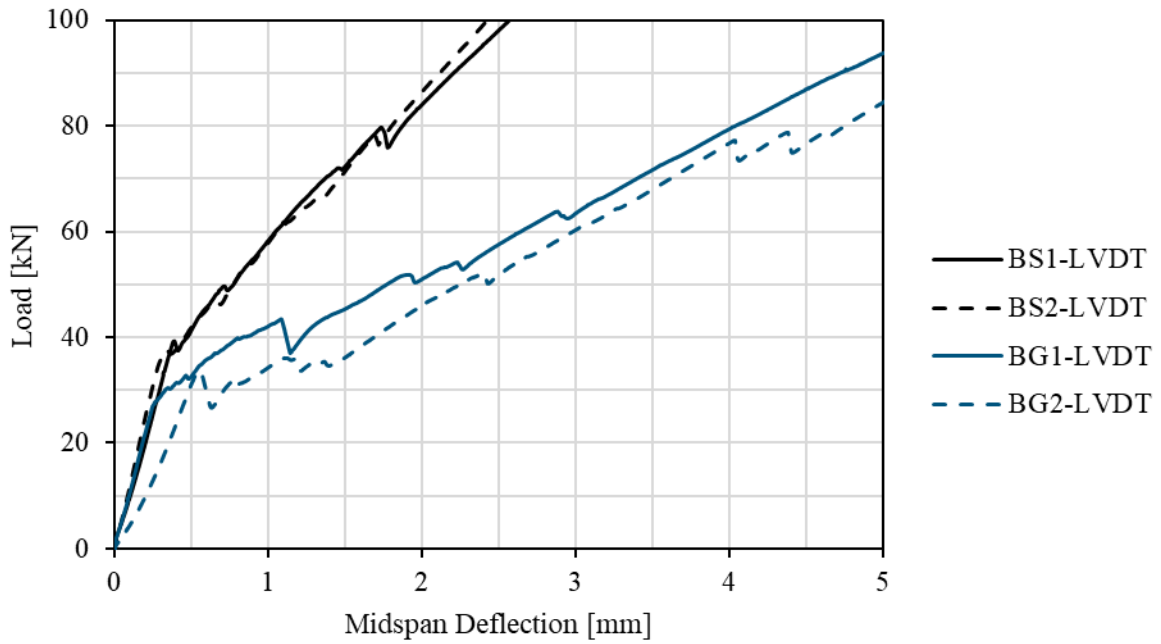
Figure 5: Load-Midspan Deflection relationship measured by
displacement transducer (LVDT) up to 100 kN and 5 mm

Results of measurement by photogrammetry

Compared to inductive displacement transducers, photogrammetry detects the complete surface of the
specimen. The load-related deformations are recorded for the duration of the test using a stochastic
pattern. The observation of a point in the centre of the beam at 0.75 m serves to validate the
measurement results of the inductive displacement transducer, which is positioned centrally below the
beam in relation to the width of the span and the component. The results of the GOM measurement are
shown in Figure 6 with a solid line. The results of the inductive displacement transducer are shown in
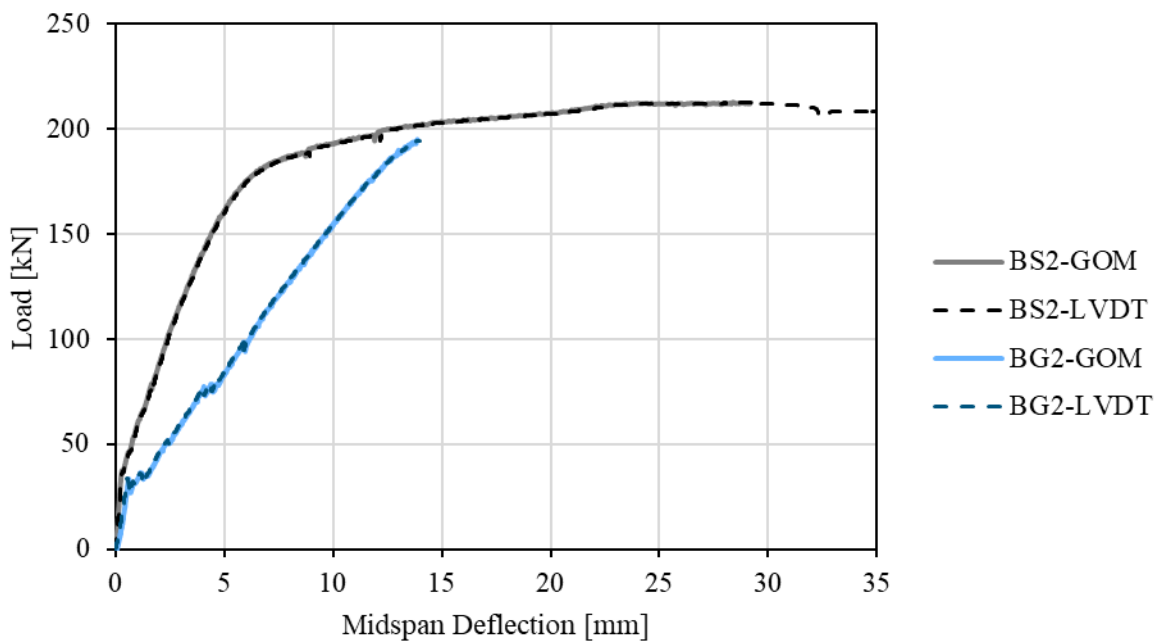Figure 6 with a dashed line.

Figure 6: Load-Midspan Deflection relationship measured by
displacement transducers (LVDT) and photogrammetry (GOM)

The plot shows that both measuring systems deliver the same result and that the curves of the component BS2 and BG2, considered separately, are exactly on top of each other.

Results on cracking

Results of measurement by photogrammetry

The result of the GOM measurement is the determination of the strains, which are recorded 2-dimensionally by the stochastic pattern over the entire face of the beam. Table 4 shows the results of the photogrammetry of the stainless steel reinforced beam BS2 and the GFRP reinforced beam BG2 for the loads 20, 40, 60 and 80 kN. On the right side of Table 4, a colour scale indicates the colour scheme of the measured strains from 0 %, shown in blue, to 0.5 %, shown in red.

Table 4: Strain photogrammetry images at four selected load levels with scale of strain in %
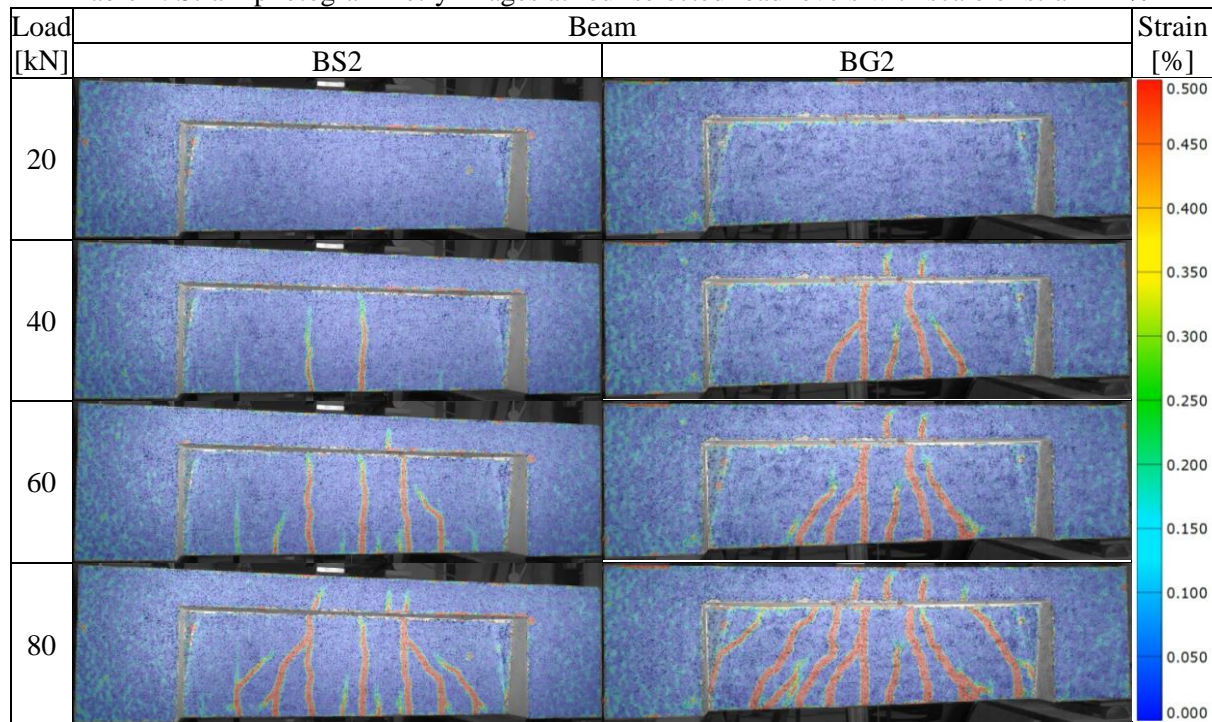
At the load level of 20 kN, the images of BS2 and BG2 show that the rebar is not elongated, which is in agreement with the data from Table 3, according to which the load at the formation of the initial crack is 37.59 kN for BS2 and 33.70 kN for BG2.

At 40 kN, two cracks can be seen in the centre of component BS2, as well as other cracks whose elongation is approx. 0.25 %. Two cracks already have a length that corresponds to the height of the reduced cross-section of 300 mm. Component BG2, on the other hand, already shows a branched crack pattern at 40 kN in the centre of the component, whereby the crack length is more than 300 mm or almost the entire height of the component. The cracks have a smaller spacing compared to BS2 at 40 kN and are partially inclined towards the centre of the component.

At 60 kN load, BS2 shows four distinctive cracks and a few small cracks running mainly vertically along the height, with cracks near the abutments in the upper area bending towards the centre. BG2 has hardly any new cracks formed compared to the 40 kN load level at 60 kN. The cracks form a detla in the centre of the beam and are almost the same length as the component height of 400 mm.

At the load of 80 kN, BS2 has a symmetrical crack pattern towards the centre of the beam, with cracks near the abutments bending obliquely towards the centre. The crack pattern of BG2 at 80 kN has changed significantly compared to 60 kN. The area where the cross-section is T-shaped is almost completely penetrated by cracks.

Results of fibre optic measurement
As shown in Figure 2, the strain of the rebar in the bending tension zone is measured by means of fibre optic measurement technology with an optical fiber glued to the rebar surface.
At the top of Figure 7 the final crack pattern of specimen BS1 is shown schematically and the location of the optical fibre is marked by a dashed line and at the bottom of Figure 7 the results of the optical fibre measurement, the strain in % versus the length of 1.50 m in mm for the load levels 20, 40, 60 and 80 kN, are shown.
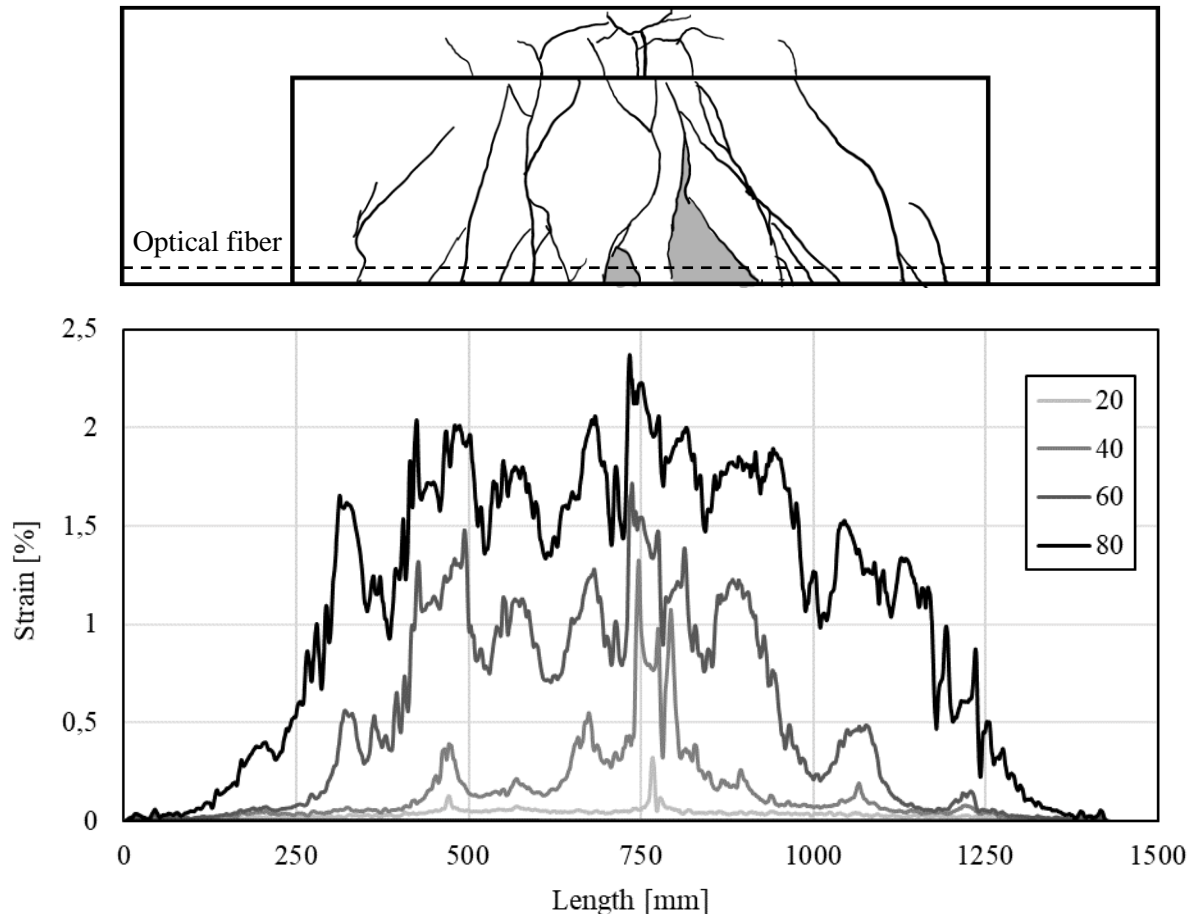

Figure 7: Crack pattern with position of optical fiber (top) and
load-related rebar strain in % over the length in mm (bottom) of beam BS1

Taking a look at the 20 kN curve first, it is noticeable in comparison to the initial crack load, which is given in Table 3 as 39.29 kN, that already at 20 kN a peak at 77 mm and 0.32 % indicates the development of the initial crack. The 40 kN curve shows multiple peaks in the centre of the element with values of 1.33, 0.98 and 1.07 %, while the rebar strain was measured less than 0.5 % except one peak at 0.55 % at 675 mm. Thus, the 40 kN curve represents the strain of the rebar as the initial crack develops. At 60 kN, the rebar is elongated over a length of more than 500 mm to such an extent that the rebar elongation is more than 0.5 %. Several peaks indicate areas of high stress and thus cracks in the beam. Only at the left abutment, between 0 and 315 mm, and at the right abutment, between 953 and 1500 mm, is the rebar strained less than 0.5 %. The 60 kN graph shows the largest peak at 1.71 % and 737 mm. At 80 kN, the bar strains have increased with the largest peak at 2.37 % and 734 mm. The rebar is elongated more than 0.5 % at almost every point in the middle of the span, i.e. between 250 and 1250 mm.

Overall, the strain curves of the BS1 component are characterised by distinct peaks, that indicate the location of cracks, and dips, that indicate the areas where the concrete is contributing to the load transfer.

By comparing the strain curve of the fibre optic measurement with the crack pattern, the peaks can be assigned to the cracks. Highly stressed rebar areas indicate failure of the concrete cover. No external cracks are visible at the beam abutments, where the strain of the rebars is low at all observed load levels.

Figure 8 schematically shows the final crack pattern after the failure of BG1 and the location of the optical fibre in the upper picture and gives the bar strain over the GFRP rebar length of 1500 mm for the load levels 20, 40, 60 and 80 kN.
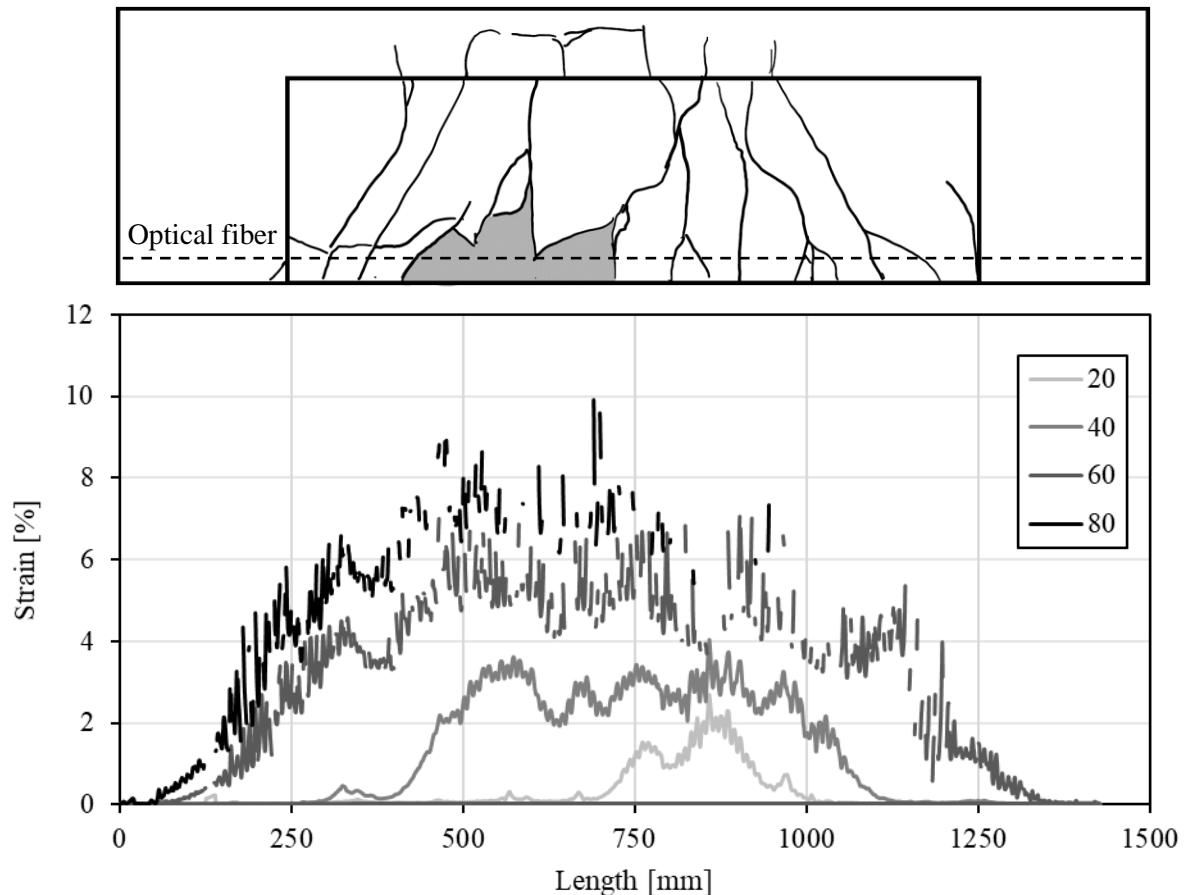

Figure 8: Crack pattern with position of optical fiber (top) and
load-related rebar strain in % over the length in mm (bottom) of beam BG1

The rebar strain at 20 kN load is only higher than 1 % in the section between 742 mm and 923 mm. The strain is maximum at 2.69 % and 859 mm. The 40 kN curve shows that the rebar is now over 1% elongated over a range of 611 mm, between 439 and 1050 mm. The average strain over this length of 439 mm is 2.62 %. On average, the strains are 1.19 % over the length of 1500mm with a maximum of 4.03 % at 859 mm. Further loading of the specimen up to 60 kN causes individual failures, whereby locally the maximum limit value of the permissible strain of the optic fibre is exceeded. The rebar is strained over the entire length at this load, so that at any point the strain is higher than 0 %. At 80 kN load, the optical fiber fails completely from 855 mm length. The maximum is 9.58 % at 700 mm.

At lower loads of 20 and 40 kN, the four curves are characterized by a smooth shape without distinctive peaks. At higher loads of 60 and 80 kN, the curve is incomplete because individual points or entire parts of the optical fibre fail due to the permissible strain limit being exceeded. The curve is characterized by closely spaced peaks where the bar is strained over the entire length.

The comparison of the fiber optic measurements and the final crack pattern following the occurrence of failure shows that cracks have also formed close to the abutments, which is consistent with the strain profile. The position of the individual cracks can only be predicted with sufficient accuracy from the

9

strain progression, since the rebar is also strained to approximately the same extent next to the crack edges as within the crack.

CONCLUSIONS

In this study, four beams were experimentally tested to failure in 4-point bending test. The specimens differ with respect to the flexural reinforcement. Two specimens are reinforced with a 16 mm stainless steel bar and two with a 16 mm GFRP rebar. The measurement concept includes inductive displacement transducers, fibre optic measurement technology and photogrammetry.

The load-deflection behavior of the four specimens was recorded by means of inductive displacement transducers. The stainless steel elements exhibit plastic behavior, while the BG1 and BG2 elements fail in a brittle manner after reaching the maximum load. The maximum load is 222.70 kN for BS1, 212.43 kN for BS2, 234.99 kN for BG1 and 14.50 kN for BG2.

By recording one longitudinal side of the specimen over the entire duration of testing, the load-deflection relationship of the displacement transducers could be validated on the one hand, and on the other hand, the strains and thus the cracks could be observed and discussed in relation to the load. For discussion of the results of photogrammetry and fiber optic measurement and, load levels of 20, 40, 60 and 80 kN were considered. BS2 showed few but distinct cracks in the center of the span, while BG2 showed a wide crack delta in the center of the span and long crack lengths extending to the top of the specimen even at low loads of 40 kN.

By using a optical fibre, which was bonded to the rebar of the bending tensile reinforcement, the strain of the rebar is measured over the entire length of the beam. While the load-related curves of component BS1 show distinctive peaks which, by comparing them with the crack pattern, correspond to the positions of the cracks, the GFRP rebar of beam BG1 is strained over longer sections, so that the comparison with the crack pattern does not allow any clear conclusions to be drawn about the position of cracks. At the same load, the GFRP rebar exhibits greater strains than the stainless steel rebar, which can be attributed to the lower modulus of elasticity of the rebar. Also, the smoother curve of BG1, which has no distinctive peaks, in contrast to the curve of BS1, which is characterized by distinctive peaks, suggests that the bond of the GFRP rod in the concrete is weaker than that of the stainless steel rod. An influence of the concrete cannot be assumed here, since specimens BS1 and BG1 were manufactured in the same batch.

Further investigations are necessary to verify the results.

CONFLICT OF INTEREST
The authors declare that they have no conflicts of interest associated with the work presented in this paper.

DATA AVAILABILITY
Data on which this paper is based is available from the authors upon reasonable request.

REFERENCES
Barris, C., Torres, L., Comas, J., & Miàs, C. (2013). Cracking and deflections in GFRP RC beams: An experimental study. Composites Part B: Engineering, 55, 580–590.

DIN Deutsches Institut für Normung e. V. (2010). Prüfung von Festbeton: Teil 6: Spaltzugfestigkeit von Probekörpern (DIN EN 12390-6:2010-09). Berlin. Beuth Verlag GmbH.

DIN Deutsches Institut für Normung e. V. (2019). Prüfung von Festbeton: Teil 2: Herstellung und Lagerung von Probekörpern für die Festigkeitsprüfung (DIN EN 12390-2:2019-10). Berlin. Beuth Verlag GmbH.

DIN Deutsches Institut für Normung e. V. (2021). Prüfung von Festbeton: Teil 13: Bestimmung des Elastizitätsmoduls unter Druckbelastung (Sekantenmodul) (DIN EN 12390-13:2021-09). Berlin. Beuth Verlag GmbH.

Gudonis, E., Timinskas, E., Gribniak, V., Kaklauskas, G., Arnautov, A. K., & Tamulėnas, V. (2013). FRP reinforcement for concrete structures: state-of-the-art review of application and design. Engineering Structures and Technologies, 5(4), 147–158.

Knab, F., Weber, A., & Schweinfurth, J. (2015). Sicherer Einsatz von Glasfaserbewehrung im Bauwesen. Beton- Und Stahlbetonbau, 110(12), 822–831.

Sayed-Ahmed, M., Hajimiragha, B [Babak], Hajimiragha, B [Borna], & Benmokrane, B. (2017). Bond strength of newly developed straight and bent glass FRP-reinforcement bars. In Internation Conference on Durability of Fiber reinforced polymer (FRP) composites for construction and rehabilitation of structures, Sherbrooke.